Towards validating stent induced micro flow patterns in left main coronary artery bifurcations

Sina Masoud-Ansari[1], John Ormiston[2], Mark Webster[2], Beau Pontre[1], Brett Cowan[1], and Susann Beier[3]

Abstract— **We investigated if blood flow changes induced through the presence of a stent could be detected using *in vitro* dynamically scaled 4D Phase-Contrast Magnetic Resonance Imaging (PC-MRI). Using idealized and patient-specific left main coronary artery bifurcations, we 3D-printed the dynamically large scaled geometries and incorporated them into a flow circuit for non-invasive acquisition with a higher effective spatial resolution. We tested the effects of using non-Newtonian and Newtonian fluids for the experiment. We also numerically simulated the same geometries in true scale for comparison using computational fluid dynamics (CFD). We found that the experimental setup increased the effective spatial resolution enough to reveal stent induced blood flow changes close to the vessel wall. Non-Newtonian fluid replicated all of the flow field well with a strong agreement with the computed flow field ($\mathbf{R}^2 > 0.9$). Fine flow structures were not as prominent for the Newtonian compared to non-Newtonian fluid consideration. In the patient-specific geometry, arterial non-planarity increased the difficulty to capture the near wall slow velocity changes. Findings demonstrate the potential to dynamically scale *in vitro* 4D MRI flow acquisition for micro blood flow considerations.**

I. INTRODUCTION

Hemodynamic flow has been a well recognized driver of pathological responses in the cardiovascular system through triggering endothelial cell behaviour and the release of inhibitors. Particularly, arterial sites exposed to hemodynamic metrics including low and high Wall Shear Stress (WSS), WSS gradient (WSSG) and Oscillatory Shear Index (OSI) are associated with intima-media thickening, thrombus development and atherosclerosis plaque location. Consequently, blood flow measurements with medical imaging have had an increasing interest in recent years, with the aim of delivering accurate, fast, and high resolution blood flow information.

The medical research field of aneurysm has made significant advancements in this regard due to better imaging accessibility and resolution compared to other less accessible vessel structures such as the coronaries [1, 2]. To make similar progress for the latter, *in vitro* efforts have been used previously, using mock loop experimental setups in combination with particle image velocimetry (PIV) flow measurements [3, 4]. The gold-standard for non-invasive flow assessment is 4D flow MRI however. MRI has not been applied to coronary flow before because of limited temporal and spatial resolution. Previously we successfully used dynamically scaled *in vitro* coronary blood flow experiments to over-come these imaging limitations [5]. In this study, we explore if the same methodology is sufficiently adequate to capture changes to blood flow on the micro scale that are a result of stents in coronary arteries. The importance of non-Newtonian properties are well known for hemodynamic assessments in coronary arteries. To the authors knowledge this has not been considered experimentally to date and thus we will consider its effects here too.

*This work was financially supported by the Auckland Charitable Heart Trust, the Auckland Medical Research Foundation (AMRF) and the Auckland Academic Health Alliance (AAHA).

[1] S.M., B.P. and B.C. are with the University of Auckand, New Zealand

[2] J.O. and M.W. are with the Auckland City Hospital¡ New Zealand

[3] S. Beier is the corresponding author and is with the Department of Mechanical and Manufacturing Engineering, University of New South Wales, Syndey, Australia s.beier{@*unsw.edu.au*

II. METHODS

To investigate if stent induced micro flow disturbances could be measured using an *in vitro* dynamically scaled MRI setup, we considered the blood flow in idealized and patient-specific left main bifurcation geometries. We compared the MRI measured flow fields in non-stented and identical stented phantoms. Both a Newtonian and a non-Newtonian fluid was used experimentally. The experimental and numerical methods have been previously described in [5] and [8] and are summarized here briefly.

A. Left Main Coronary Geometries

The left main coronary geometry was generated from an individual patient imaged using computed tomography coronary angiogram (CTCA). The patient provided written informed consent under the institutional ethics committee approval for the use of the images. The patient had a calcium core of zero and no stenosis. The images were obtained using a multi-detector CT scanner (GE Lightspeed 64) with retrospective electrocardiogram (ECG) gating after administration of beta blockers for a resting heart rate of approximately 60 bpm. Only the end-diastolic CT images were rendered to construct the 3D representation [10].

The image stack was segmented by an experienced analyst using the seed growth method in Osirix (v. 4.1.2) and the CMIV CTA plug-in to generate the vessel centerlines [11]. The lumen was smoothed using Poisson surface reconstruction, cut and rendered and extended in the open-source VMTK software (Vascular modelling tool kit, www.vmtk.org) as detailed in an earlier publication [5]. The virtual geometry was then imported into AutoCAD Inventor (2016, AutoDesk, SanRafael, CA, USA).

The idealized geometry was simplified, having a 4.2 mm straight inlet representing the left main branch, and the daughter vessels with 3.3 mm diameter each (obeying

978-1-5386-1311-5/19/$31.00 ©2019 IEEE

Murray's Law) branching off symmetrically in the same plane in a 40° angle.

A representation of the BioMatrix stent by Biosensors International Ltd. was created in AutoCAD Inventor and projected onto a copy of the patient-specific and idealized vessel bifurcation in all branches to resemble an idealized deployment with perfect 50% cross-sectional vessel penetration as detailed in [12]. Tissue prolapse was ignored.

B. 4D MRI Flow measurement

The virtual vessel geometries were scaled from an inlet diameter of 4 mm to 25 mm, representing a six-fold increase. These were then 3D printed using a Project 3500 HD Plus 3D Printer (VisiJet-X plastic material, 3D Systems, Valencia, CA) resulting in a rigid, 16 μm layer and 25 - 50 μm resolution replica. Fig. 1 shows the inside of the 3D printed idealized stented vessel.

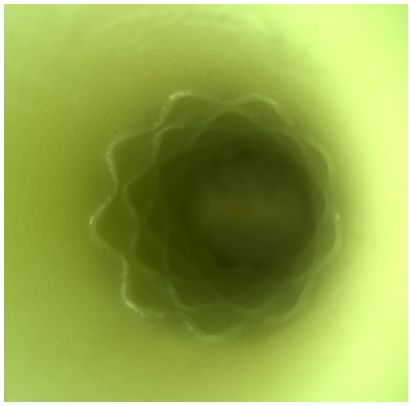

Fig. 1. Inside of the 3D printed vessel showing the replicated stent geometry.

The 3D printed vessels were incorporated into a flow circuit comprised of PVC hosing, a flow reservoir, flow meter, pressure control valve and steady flow pump. The fluid flow in the phantom was imaged on a 3T Skyra MRI system (Siemens, Erlangen, Germany) with a 16-channel body array coil placed over the phantom for signal detection. A 4D phase contrast sequence was used for images acquisition with the following scan parameters: TR = 425.04 msec, TE = 4.64 msec, flip angle = 158°, voxel size 1.0 x 1.0 x 1.0 mm, with the velocity encoding (VENC) set to 30, 40 and 100 cm/s (through-plane, left-right and head-foot directions, respectively). Total acquisition time was 27:54 minutes.

To mimic blood shear thinning behaviour we used a aqueous xanthan gum solution which we produced with a high shear rate industrial mixer to guarantee a homogeneous mix [9].

Dynamic similarity was achieved by matching the dimensionless Reynolds number calculated as

$$Re = \frac{\rho v_{mean} d}{\mu_{mean}} \quad (1)$$

where ρ is the density, which was 1060 and 989 kg/m^3 for blood and xanthan gum solution respectively, v is the dynamic viscosity evaluated at the inlet, μ_{mean} is the mean velocity, and d is the proximal diameter as listed in Table 1.

TABLE I
EXPERIMENTAL SETUP WITH DYNAMIC SCALING COMPARED TO DYNAMIC RANGE EXPECTED IN VIVO

	Diameter d (mm)	Velocity v_{mean} (m/s)	Viscosity μ_{mean} (m^2/s)	Density ρ (kg/m^3)	Reynolds Re (-)
In vivo	4.2	0.6	0.0035	1060	540
In vitro	25	0.77	0.0350	989	540

Results were compared using MATLAB (R2016a, MathWorks, Natick, MA).

C. CFD Simulation

The creation of the virtual geometries allowed the import into the commercial CFD software ANSYS (v. 17). The true scale geometries where meshed in ANSYS mesher module (Canonsburg, PA, USA) using a patch-conforming, unstructured tetrahedral mesh. A sensitivity test comprised approximately 8 million elements before solving the fluid domain in CFX on a high-performance parallel computing cluster (64-bit 2.7 GHz Intel Xeon, 8 nodes, 60 CPU, 40 GB RAM). Navier-Stokes equations with 'no slip' boundary conditions (zero velocity) were used at the vessel walls. Vessel walls were assumed to be rigid to enable comparison with the stiff PC-MRI phantoms. The shear thinning behavior of blood was accounted for with the non-Newtonian 'Carreau-Yasuda' model. A constant static pressure condition was prescribed at the two outlets. The experimentally measured MRI inlet profile was prescribed as the inlet velocity profile in the CFD.

III. RESULTS AND DISCUSSION

A. Dynamically scaled 4D Flow MRI captured micro flow structures

Micro flow disturbances introduced by the presence of the stent were captured well in the idealized geometry with non-Newtonian fluid as shown in Fig. 2. The Newtonian experiment only minimally captured the flow changed induced through the stent. The patient-specific geometry dominated the flow domain compared to the stent.

B. Non-Newtonian fluid properties must be accounted for

When comparing the velocity magnitudes, there was a clear difference in the stented and non-stented cases. While the flow field difference was small for Newtonian study shown in Fig. 3, the differences increased for the non-Newtonian case shown in Fig. 4. A good agreement in voxel-by-voxel velocities correspondence with $R^2 > 0.9$ was found when comparing to the CFD computation.

The flow in non-stented and stented idealized bifurcation geometries showed notable differences between blood mimicking non-Newtonian and Newtonian fluid used. The mean velocities for the non-stented case was 3.3 m/s whereas the stented case reached 3.5 m/s. This mean flow difference

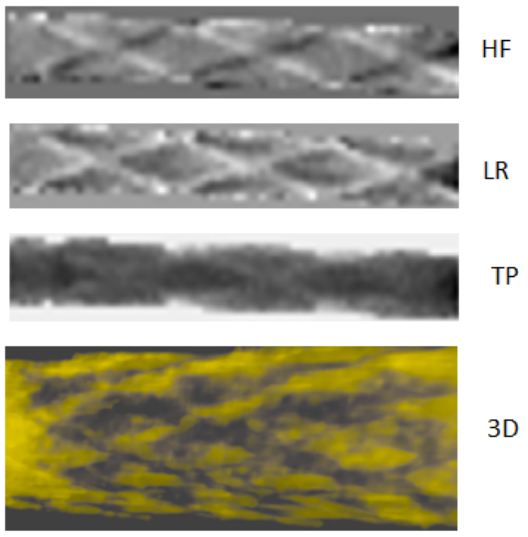

Fig. 2. Grey scale read out for all three-directional velocity components u, v and w in the head - foot (HF), left - right (LR), through - plane (TP) respectively, and the 3D reconstructed flow field at the boundary (3D) for the non-Newtonian experiment in the idealized left main coronary.

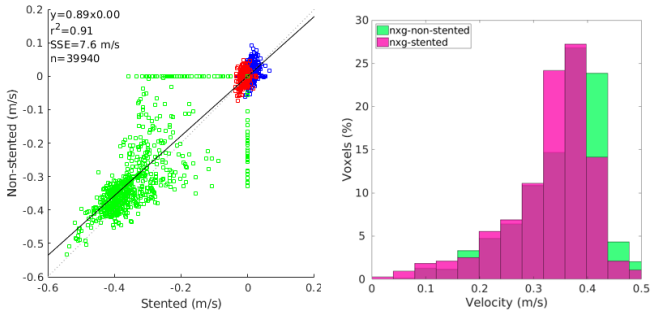

Fig. 3. Left: Three-directional flow field comparison between non-Newtonian non-stented and stented idealized geometry velocity components u as direction of main flow (green), v as left-right planar with the branching (red) and top-to-bottom (blue), with Pearsons linear correlation analysis shown for n number of voxels and Sum of Squared Error (SSE). Right: Comparison of velocities per voxel over comparable volumes near the vessel wall using non-Newtonian fluid.

increased notably when using Newtonian fluid, whereby a mean velocity of 1.9 versus 2.6 m/s was measured respectively.

A comparison between stented velocities for both the non-Newtonian and Newtonian study are shown in Fig. 5.

C. Patient-specific consideration

Quantification for the patient specific geometry was more challenging than the planar idealized geometries. The micro flow patterns do not necessarily align with the selected 2D imaging slice of the acquired MRI z-stack. The potential misalignment meant that a volume-based acquisition was required to adequately compare the MRI data to the CFD. The image segmentation approach had a significant impact on the results due to the low velocities close to the wall. In future studies we suggest to acquire a structural 3D image with no induced flow, potentially using gadolinium contrast,

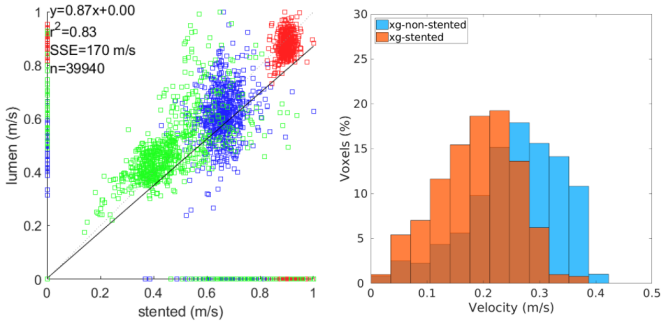

Fig. 4. Left: Three-directional flow field comparison between Newtonian non-stented and stented idealized geometry velocity components u as direction of main flow (green), v as left-right planar with the branching (red) and top-to-bottom (blue), with Pearsons linear correlation analysis shown for n number of voxels and Sum of Squared Error (SSE). Right: Comparison of velocities per voxel over comparable volumes near the vessel wall using Newtonian fluid.

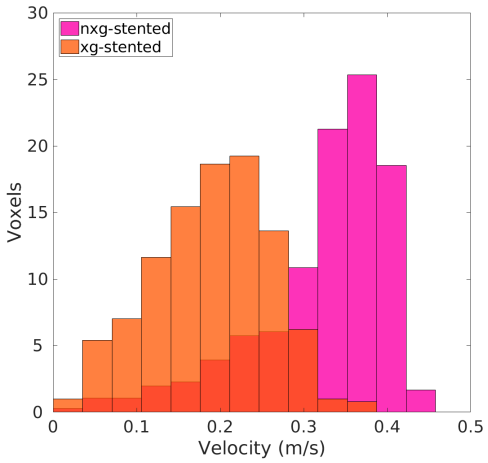

Fig. 5. Velocity comparison for both stented cases, idealized and patient-specific, using non-Newtonian properties.

during MR acquisition to mitigate the problem of 4D-flow segmentation.

Flow patterns induced by the stent where also found to be impacted by the vessel geometry, either mitigating (at the daughter branches) or amplifying (at the left main segment) it, see Fig. 6.

The pursuit for non-invasive comprehensive and accurate flow measurement is pressing and an increasing number of studies are aiming to push imaging acquisition boundaries [7]. One study managed to quantify excessive intimal thickening *in vivo* [7], yet this application may be a long way from clinical implementation for detailed real-time blood flow measurements. Whilst further developments in this field are exciting, intermediate assessments are warranted to build the foundation and insights informing such clinical implementation. The present study may contribute to such efforts and future blood flow studies may use *in vitro* dynamic scaling to overcome current resolution limitations with non-invasive imaging including 4D flow MRI [5].

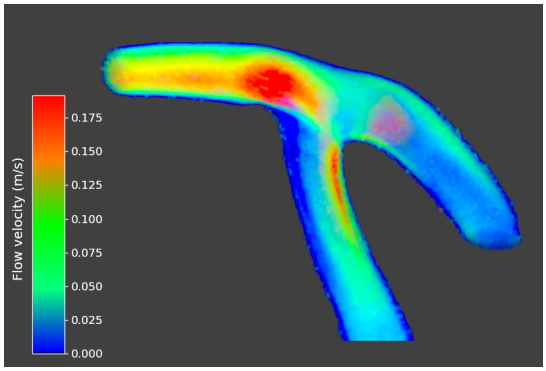

Fig. 6. Patient left main blood flow with blue, green and red indicating slow, medium and fast flow respectively.

IV. CONCLUSIONS

The study demonstrated that dynamically scaled *in vitro* 4D MRI Flow imaging can capture detailed flow dynamics induced by the presence of the stent. The use on non-Newtonian blood mimicking fluid is recommended as finer micro flow structures are captured in agreement with computational results. Patient-specific geometries were found to be more challenging when considering stent induced flow features *in vitro* because the vessel geometry dominates the local blood flow zones even at the boundary layer. Additionally, the analysis was more challenging as it requires a whole volume consideration rather slice by slice analysis, introducing larger errors due to low near wall velocities. Nevertheless the potential of capturing micro flow patterns using dynamically scaled *in vitro* MRI is demonstrated.

ACKNOWLEDGMENT

The authors thank Dr. Pau Medrano-Gracias for the image collection and Dr. Cyril Tous and Kaitlin Logie for the assistance with the data acquisitions.

REFERENCES

[1] Pereira, V.M., et al., Assessment of intra-aneurysmal flow modification after flow diverter stent placement with four-dimensional flow MRI: a feasibility study. J Neurointerv Surg, 2015. 7(12): p. 913-9.

[2] Struffert, T., et al., Measurement of quantifiable parameters by time-density curves in the elastase-induced aneurysm model: first results in the comparison of a flow diverter and a conventional aneurysm stent. Eur Radiol, 2013. 23(2): p. 521-7.

[3] Brindise, M.C., et al., Hemodynamics of Stent Implantation Procedures in Coronary Bifurcations: An In Vitro Study. Ann Biomed Eng, 2016.

[4] Engels, G.E., S.L. Blok, and W. van Oeveren, In vitro blood flow model with physiological wall shear stress for hemocompatibility testing-An example of coronary stent testing. Biointerphases, 2016. 11(3): p. 031004.

[5] Beier, S., et al., Dynamically scaled phantom phase contrast MRI compared to true-scale computational modeling of coronary artery flow. J Magn Reson Imaging, 2016. 44(4): p. 983-92.

[6] Kabinejadian, F., et al., A novel carotid covered stent design: in vitro evaluation of performance and influence on the blood flow regime at the carotid artery bifurcation. Ann Biomed Eng, 2013. 41(9): p. 1990-2002.

[7] Nagel, E., et al., Noninvasive determination of coronary blood flow velocity with cardiovascular magnetic resonance in patients after stent deployment. Circulation, 2003. 107(13): p. 1738-43.

[8] Beier, et al., Coronary Shape Biomarkers for Adverse Hemodynamic Prediction IEEE ISBI 2017.

[9] Beier, S., et al., Vascular Hemodynamics with Computational Modeling and Experimental Studies, in Computing and Visualization for Intravascular Imaging and Computer-Assisted Stenting. 2017, Elsevier. p. 227-251.

[10] Medrano-Gracia, P., et al., A Computational Atlas of Normal Coronary Artery Anatomy. EuroIntervention: journal of EuroPCR in collaboration with the Working Group on Interventional Cardiology of the European Society of Cardiology. 2016 Sep;12(7):845-54.

[11] Medrano-Gracia, P., et al., A Study of Coronary Bifurcation Shape in a Normal Population. Journal of Cardiovascular Translational Research, 2016: p. 1-9.

[12] Beier, S., Haemodynamic Assessment of Coronary Flow with CFD and Phase-Contrast MRI. Diss. University of Auckland, 2015.